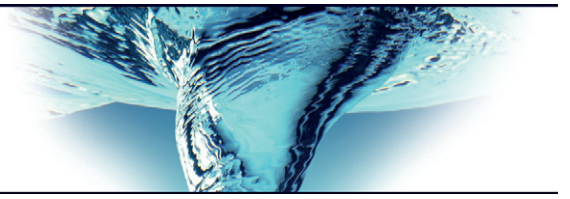
CrossMark

J. Fluid Mech. (2017), *vol.* 827, R3, doi:10.1017/jfm.2017.535



JFM RAPIDS
journals.cambridge.org/rapids

Stability of a growing cylindrical blob

R. Krechetnikov†

Mathematical and Statistical Sciences, University of Alberta, Edmonton, AB, T6G 2G1, Canada

(Received 23 June 2017; revised 1 August 2017; accepted 1 August 2017;
first published online 18 August 2017)

The stability of an accelerating cylindrical blob of a time-varying radius is considered with the goals of understanding the effects of time dependence of the underlying base state on a Rayleigh–Plateau instability as well as of evaluating a contribution due to a lateral acceleration of the blob, treated as a perturbation here. All of the key processes contributing to instability development are dissected, with analytical analyses of the exact incompressible inviscid potential flow formulation. Herein, without invoking the 'frozen' base state assumption, the entire time interval of the evolution of a perturbation is explored, discerning physical mechanisms at each stage of development. It transpires that the stability picture proves to be cardinally different from Rayleigh's standard analysis.

Key words: instability, interfacial flows (free surface)

1. Introduction

Breakup of a time-varying cylindrical blob represents a key example of the evolution of a perturbation superimposed on a time-dependent base state and arises in various situations, such as edges of retracting soap films, extending fluid threads and stretching liquid bridges. Historically, proper stability analysis of time-dependent base states has often been obstructed by the difficulties associated with analytical treatment, apart from very few scarce exceptions when there is symmetry (Plesset 1954) or periodicity (Davis 1976), and is therefore most frequently amenable to numerical methods only (Homsy 1973). Without exception, stability analysis of a growing blob has hitherto been based on either phenomenological (i.e. not exact) formulations or numerical simulations (cf. Fullana & Zaleski (1999), Roisman, Horvat & Tropea (2006), Agbaglah, Josserand & Zaleski (2013), Dziwnik *et al.* (2014), to name a few), often producing contradictory results and thus calling for a precise analysis to be performed. Explicit in many of these studies is the universal assumption that the instability can be described by spectra (eigenvalues) of the corresponding autonomous linear operator, usually enabled by a 'frozen' base state, resulting in exponential growth of the perturbation. A somewhat different formulation

† Email address for correspondence: krechet@ualberta.ca

© Cambridge University Press 2017

https://doi.org/10.1017/jfm.2017.535 Published online by Cambridge University Press

by Dziwnik *et al.* (2014), based on a thin-film approximation, which strictly speaking is invalid in the rim region and in which the initial fronts evolve slower compared with their instability, thus allowing a time-scale separation, envisaged the idea of a time-dependent dominant wavelength that scales with the size of the growing rim.

As will be shown in the present study (§ 3), the assumption of exponential growth proves to be inadequate in the context of a growing rim if its (base sate) radius varies on the same time scale as instability. Moreover, the results of the analysis of the original fluid dynamics equations (§§ 2–3) suggest that the phenomenological equations fail to capture the true intricacies of the instability dynamics. It is also demonstrated that the seemingly intuitive idea of a time-dependent wavenumber scaling with the time-dependent rim radius is not mathematically justified (§ 3). For an analytical study of the instability of an accelerating cylindrical blob in the large-Bond-number regime, when its growth in time is treated in a quasi-steady fashion (i.e. instability develops faster than the initial cylindrical base state is modified), the reader is referred to Krechetnikov (2010). In the present work, we consider the opposite situation, namely when the time dependence of the base state (growing cylinder) cannot be neglected, but the effect of the lateral acceleration g is treated as a perturbation in the limit of small Bond number.

2. Derivation of the linear stability equations

The problem of breakup of a liquid jet is often studied in the incompressible inviscid potential approximation, starting with the work of Rayleigh (1878) and continuing with more recent studies (Agbaglah *et al.* 2013), which allows one to explain the breakup phenomena robustly. Adopting this formulation, the governing equations for a fluid of density ρ and surface tension σ reduce to the Laplace equation for the velocity potential ϕ, the Cauchy–Lagrange integral for the pressure p and the kinematic boundary condition at the cylinder interface $r = f(t, z, \vartheta)$ (cf. figure 1*a*):

$$\Delta\phi = 0, \quad \text{for } r \leqslant f(t, z, \vartheta), \tag{2.1a}$$

$$\frac{\partial\phi}{\partial t} + \frac{1}{2}|\nabla\phi|^2 = -\frac{1}{\rho}p + gy + C(t), \quad \text{for } r \leqslant f(t, z, \vartheta), \tag{2.1b}$$

$$\frac{\partial f}{\partial t} = \frac{\partial\phi}{\partial r} - \frac{1}{r^2}\frac{\partial\phi}{\partial\vartheta}\frac{\partial f}{\partial\vartheta} - \frac{\partial\phi}{\partial z}\frac{\partial f}{\partial z}, \quad \text{at } r = f(t, z, \vartheta). \tag{2.1c}$$

Here, $C(t)$ is an arbitrary function of time which can be added to ϕ without changing the velocity field $\boldsymbol{v} = \nabla\phi$. The cylinder interface $S = r - f(t, z, \vartheta)$ is characterized by the unit normal vector $\boldsymbol{n} = \nabla S/|\nabla S|$ and the interfacial curvature, which simplifies to $\nabla \cdot \boldsymbol{n} \simeq r^{-1} - f_{zz} - r^{-2}f_{\vartheta\vartheta}$ for small departures from a circular cylinder shape. The cylinder is accelerated in the y-direction with a magnitude $g = |\boldsymbol{g}|$. Following the classical treatment (Drazin & Reid 2004), we perform analysis in dimensional variables, except for the numerical results to be presented in § 3.1, which for convenience are in a non-dimensional form.

2.1. *Base state*

We will study stability of the axisymmetric uniform (i.e. with pure radial growth) cylinder base state, which does not depend on the z and ϑ coordinates: $\phi = \Phi(t, r)$, $p = P(t, r)$, $f = F(t)$. It is straightforward to show from the structure of equations (2.1)

https://doi.org/10.1017/jfm.2017.535 Published online by Cambridge University Press

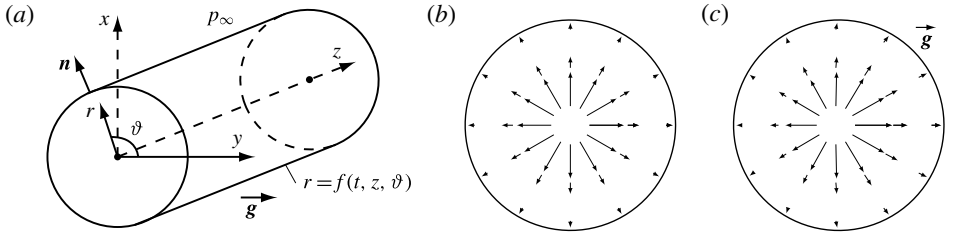


FIGURE 1. On stability of a cylindrical blob: (*a*) problem set-up, (*b*,*c*) qualitative velocity fields of the base state without (*b*) and with (*c*) the lateral acceleration $\boldsymbol{g}$. The vector lengths show the relative velocity magnitudes.

that this is possible only if there is no flow in the z-direction and $g = 0$. Since we are going to consider the case $Bo = \rho g F^2/\sigma \ll 1$, then deviation from this base state due to acceleration can be treated as a perturbation (§ 4.1). The Laplace equation (2.1*a*) admits a non-trivial solution of the above type only when there is a line source at the axis of symmetry providing a mass flux Q, treated here as constant,

$$\Phi(t, r) = (Q/2\pi)\ln r, \tag{2.2}$$

producing an axisymmetric flow field; cf. figure 1(*b*). The logarithmic singularity can be removed by considering a mass source on the cylinder axis of a small radius $\epsilon > 0$. The time-dependent cylinder radius $F(t)$ is found from the kinematic boundary condition (2.1*c*), yielding $F(t) = \sqrt{F_0^2 + Qt/\pi}$, the same as the rim growth on a retracting soap film in the Taylor–Culick theory (Taylor 1959; Culick 1960). We will focus, without loss of generality, on the asymptotic case,

$$F(t) \simeq \sqrt{Qt/\pi}, \quad \text{valid for } t \gg \pi F_0^2/Q \equiv t_c. \tag{2.3}$$

For a shrinking cylinder, i.e. when $t' = t_c - t \ll t_c$, $F(t) \simeq \sqrt{Qt'/\pi}$, and since $\partial_t \to -\partial_{t'}$, the stability results would be the exact opposite of the case considered below. The base state pressure is $P(t, r) = p_\infty + \sigma \boldsymbol{\nabla} \cdot \boldsymbol{n} = p_\infty + \sigma/r$, so that the constant $C(t)$ determined by evaluating the Cauchy–Lagrange integral (2.1*b*) at the cylinder surface $r = F(t)$ becomes $C(t) = \sigma/\rho F(t) + (Q/2\pi F)^2/2$. Then, deviations from this base state due to instability development and lateral acceleration can be treated as perturbations in §§ 3 and 4, respectively.

2.2. *Perturbation equation*

In the analysis to follow, first, we are going to superimpose general perturbations of the form $f(t, z) = F(t) + f'(t, \vartheta, z)$, $\phi(t, r) = \Phi(t, r) + \phi'(t, \vartheta, r)$, $p(t, r, \vartheta) = P(t, r) + p'(t, r, \vartheta)$. Due to the linearity of inviscid incompressible potential flows, the perturbation of the velocity potential ϕ' obeys the Laplace equation (2.1*a*) as well. Following the same procedure as in the classical case (Drazin & Reid 2004), modulo the time-dependent boundary $r = F(t)$, the linearization of the kinematic condition (2.1*c*), after projecting onto the undisturbed interface $r = F(t)$ and taking into account that $\Phi_r|_{r=F+f'} = \Phi_r|_F + \Phi_{rr}|_F f' + \text{higher-order terms}$, furnishes

$$r = F(t) : \frac{\partial f'}{\partial t} = \left.\frac{\partial^2 \Phi}{\partial r^2}\right|_F f' + \frac{\partial \phi'}{\partial r}. \tag{2.4}$$

https://doi.org/10.1017/jfm.2017.535 Published online by Cambridge University Press

Similarly, we can linearize the dynamic condition (2.1*b*) around $r = F(t)$,

$$\frac{\partial \phi'}{\partial t} + \frac{\partial \Phi}{\partial r}\left(\frac{\partial^2 \Phi}{\partial r^2} f' + \frac{\partial \phi'}{\partial r}\right) = -\frac{1}{\rho}[p|_{r=F+f'} - P|_{r=F}] + g\cos\vartheta\,(F(t) + f'), \tag{2.5}$$

where the expression in square brackets simplifies given the pressure perturbation at the interface $p' = -\sigma\,(f_{zz} + f_{\vartheta\vartheta}/F^2(t))$ related to the perturbed part of the interfacial curvature $\boldsymbol{\nabla \cdot n}$,

$$[\cdots] = \left[\left.\frac{\partial P}{\partial r}\right|_{r=F} f' + p'\right] = -\left.\frac{\sigma}{r^2}\right|_{r=F} f' + p' = -\sigma\left(\frac{f' + \partial^2 f'/\partial\vartheta^2}{F^2(t)} + \frac{\partial^2 f'}{\partial z^2}\right). \tag{2.6}$$

It should be noted that when calculating $\partial\Phi/\partial t$ in (2.1*b*), we first differentiate (with respect to time t) and then evaluate at $r = F(t)$, not *vice versa* – these two operations do not commute. The same result (2.5) can be arrived at directly from Euler's equations of fluid motion.

Taking an infinite Fourier transform in the z-direction and a finite Fourier transform in the ϑ-direction, the Laplace equation (2.1*a*) reduces to $r^{-1}\partial_r(r\widehat{\phi}'_r) - (k^2 + n^2/r^2)\widehat{\phi}' = 0$, with the solution expressed in terms of the modified Bessel functions $\widehat{\phi}'_n = C_n I_n(kr) + D_n K_n(kr)$, where k and n are continuous axial and discrete (i.e. quantized due to boundedness of the ϑ domain) azimuthal wavenumbers, respectively. Thereby, the conditions (2.4) and (2.5) become

$$\begin{aligned} r = F(t) : \frac{\partial}{\partial t}\begin{pmatrix}\widehat{f}'_n \\ \widehat{\phi}'_n\end{pmatrix} &= \begin{pmatrix} \Phi_{rr} & \dfrac{\partial}{\partial r} \\ -\Phi_r\Phi_{rr} + \dfrac{\sigma}{\rho}\left(\dfrac{1-n^2}{F^2(t)} - k^2\right) & -\Phi_r\dfrac{\partial}{\partial r}\end{pmatrix}\begin{pmatrix}\widehat{f}'_n \\ \widehat{\phi}'_n\end{pmatrix} \\ &+ \frac{g}{2}\begin{pmatrix}0 \\ \widehat{f}'_{n-1} + \widehat{f}'_{n+1}\end{pmatrix} + \frac{gF}{2}\begin{pmatrix}0 \\ \delta_{n,-1} + \delta_{n,1}\end{pmatrix}, \end{aligned} \tag{2.7}$$

where $\delta_{n,m}$ is the Kronecker delta function. As we can see from the above system, the base state is affected by acceleration g only at the mode $n = 1$. Moreover, since the system (2.7) is symmetric with respect to the transformation $n \to -n$, in the subsequent stability analysis we can focus on $n \geqslant 0$. The system (2.7) is universal in the sense that it allows us to compute both distortion of the base state from a circular cylinder state and the time-dependent perturbation responsible for instability (or stability); in the former case, the amplitude of the distortion is limited by the magnitude g of acceleration, while in the latter case, the amplitude can grow unboundedly.

Modes corresponding to the modified Bessel functions of the first kind I_n play the dominant role in the instability, since the K_n are singular at $r = 0$ and decay towards the cylinder surface, where the instability is driven by the surface tension forces. Hence, we can put $D_n = 0$ as in the classical case of a time-independent cylinder (Drazin & Reid 2004). If the line source is substituted (to remove the singularity at $r = 0$) by a finite-size mass source $r \leqslant \epsilon$, then the K_n would need to be taken into account, but for $\epsilon \ll 1$ their contribution should be negligible for the above reasons. With these considerations, we can reduce the system (2.7) to a single second-order equation. From the first equation of (2.7), we determine $C_n = [\mathrm{d}\widehat{f}'_n/\mathrm{d}t - \Phi_{rr}(F)\widehat{f}'_n]/kI'_n(kF)$, where we divided by $I'_n(kF)$ since it does not have

https://doi.org/10.1017/jfm.2017.535 Published online by Cambridge University Press

zeros for $kF \geqslant 0$, and substituting into the second of equations (2.7) we arrive at a second-order equation for $\widehat{f}'_n$,

$$L\widehat{f}'_n = \frac{\mathrm{d}^2\widehat{f}'_n}{\mathrm{d}t^2} + a(t)\frac{\mathrm{d}\widehat{f}'_n}{\mathrm{d}t} + b(t)\widehat{f}'_n = \frac{g}{2}(\widehat{f}'_{n-1} + \widehat{f}'_{n+1}) + \frac{gF}{2}(\delta_{n,-1} + \delta_{n,1}), \tag{2.8}$$

with the coefficients defined by

$$a(t) = -\Phi_{rr}(F) - k\frac{I''_n(kF)}{I'_n(kF)}\frac{\mathrm{d}F}{\mathrm{d}t} + k\frac{I'_n(kF)}{I_n(kF)}\Phi_r(F), \tag{2.9a}$$

$$b(t) = -\Phi_{rrr}(F)\frac{\mathrm{d}F}{\mathrm{d}t} + k\frac{I''_n(kF)}{I'_n(kF)}\frac{\mathrm{d}F}{\mathrm{d}t}\Phi_{rr}(F) - k\frac{I'_n(kF)}{I_n(kF)}\frac{\sigma}{\rho}\left(\frac{1-n^2}{F^2} - k^2\right). \tag{2.9b}$$

3. Stability analysis for $g = 0$

3.1. *Numerical integration of the evolution equation*

In order to get an initial insight into the solution of (2.8), let us non-dimensionalize it for the convenience of numerical integration only. Letting $t = t_0\widetilde{t}$ with $t_0 = \sqrt{\rho F_0^3/\sigma}$ (surface-tension-driven breakup time for a cylinder of radius F_0), (2.8) reduces to

$$\frac{\mathrm{d}^2\widehat{f}'_n}{\mathrm{d}\widetilde{t}^2} + \widetilde{a}(\widetilde{t})\frac{\mathrm{d}\widehat{f}'_n}{\mathrm{d}\widetilde{t}} + \widetilde{b}(\widetilde{t})\widehat{f}'_n = 0, \tag{3.1a}$$

where

$$\widetilde{a}(\widetilde{t}) = \frac{\widehat{a}(\kappa)}{2\widetilde{t}}, \quad \widetilde{b}(\widetilde{t}) = -\frac{1}{4\widetilde{t}^2}[2 + \widehat{b}_2(\kappa)] - \widehat{b}_1(\kappa)\left(\frac{t_*}{t_0}\right)^{3/2}\frac{1-n^2-\kappa^2}{\widetilde{t}^{3/2}}, \tag{3.1b,c}$$

with the abbreviations $\widehat{b}_1(\kappa) = \kappa I''_n(\kappa)/I'_n(\kappa)$, $\widehat{b}_2(\kappa) = \kappa I'_n(\kappa)/I_n(\widehat{k})$, $\widehat{a}(\kappa) = 1 + \widehat{b}_2(\kappa) - \widehat{b}_1(\kappa)$ and the non-dimensional wavenumber $\kappa = \widehat{k}\widetilde{t}^{1/2}$. Here, $\widehat{k} = \widetilde{k}(t_0/t_*)^{1/2}$, $\widetilde{k} = kF_0$ and the inertial time scale $t_* = \pi F_0^2/Q \equiv t_1$ (which can be interpreted as the time to grow from $F = 0$ to F_0). Thus, the solution $\widehat{f}'_n$ of (3.1*a*) can be treated as a function of $\widetilde{t}$, n and $\widehat{k}$.

If one naively applies the stability results for a time-independent cylinder to a time-dependent one, it seems to be intuitive to hypothesize that the most unstable wavenumber should still scale as $k \sim F^{-1}$, now being time-dependent. Indeed, after analysing equations (3.1) with $\kappa = \text{const.}$, we conclude that for large time, $\widetilde{t} \to \infty$, the solution behaves as

$$\widehat{f}'_0 \sim \widetilde{t}^{-\widehat{a}(\kappa)/4-(1/8)}\mathrm{e}^{4\sqrt{c}\,\widetilde{t}^{1/4}}, \quad c = \widehat{b}_2(\kappa)(1-\kappa^2)(t_*/t_0)^{3/2}. \tag{3.2a,b}$$

For truly $\widetilde{t} \to +\infty$, the growth is dominated by the exponential only, so that the maximum growth rate is achieved when $c(\kappa)$ is at maximum, which occurs at some finite $\kappa = O(1)$ similar to the classical dispersion relation (3.5); cf. also figure 1.5 of Drazin & Reid (2004). For finite times, the optimum κ is affected by $a(\kappa)$ as well. The problem with the above hypothesis $k \sim F^{-1}$ is that it implicitly requires the Fourier transform with time-dependent wavenumber to commute with the operation of the time derivative, whereas they clearly do not. Hence, it can be surmised that the hypothesis is not viable. In fact, by solving an initial value problem for (3.1*a*),

https://doi.org/10.1017/jfm.2017.535 Published online by Cambridge University Press

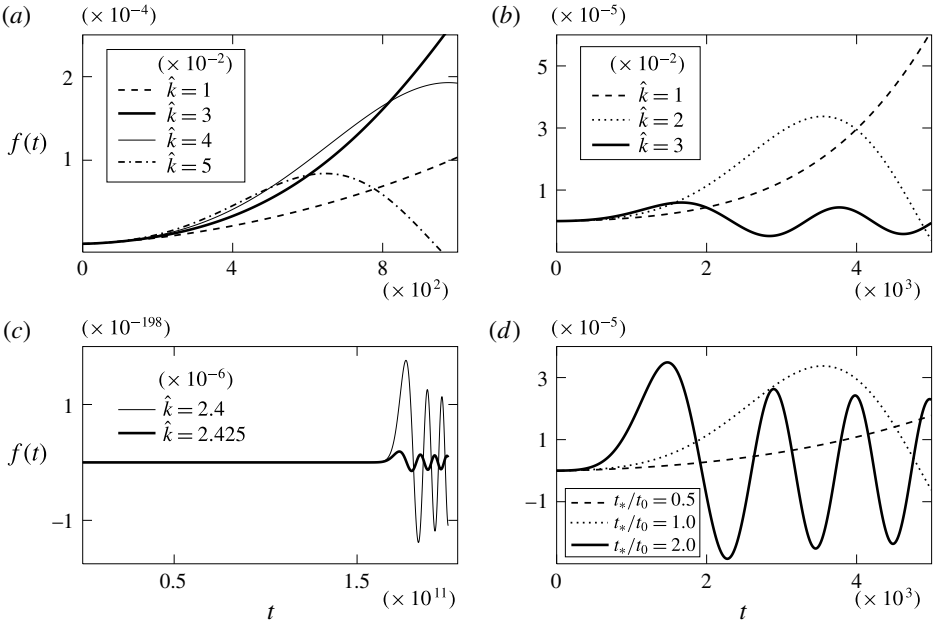


FIGURE 2. Plots of $\widehat{f}_n'$ at different wavenumbers $\widehat{k} \in [0, 0.1]$ for $n = 0$ and $t_*/t_0 = 1$: (*a*) short time interval; (*b*) longer time interval; (*c*) ultra-long time interval with ultra-short wavenumbers $\widehat{k} = O(10^{-6})$; (*d*) solution for $\widehat{k} = 2 \times 10^{-2}$ from figure 2(*b*) for three values of t_*/t_0.

we can validate this suspicion. Before that, let us first make a few observations from numerical solution of (3.1), which can be constructed accurately even for long times using the conservative nature of the problem at hand and hence appealing to symplectic integrator methods.

From figure 2(*a*), the mode entanglement makes it clear that the growth is not monotonic with the wavenumber k and time t. Moreover, what appears to be a 'winning' mode (bold) on a short time interval becomes a decaying oscillating mode on a longer time interval; cf. figure 2(*b*). It also appears, cf. figure 2(*c*), that there is no short-wavenumber cutoff – the limit $k \to 0$ indicates that the perturbation starts to grow at a very long time and brings up larger maxima of the solution $\widehat{f}_0'$ compared with shorter wavelengths. The latter observation suggests that there is no optimal, i.e. most amplified, wavenumber, as the maximum achieved increases with decreasing k. Any wavenumber k, no matter how small, is eventually amplified and then damped; cf. figure 2(*c*). Finally, as observed from figure 2(*d*), increase of the inertial over the surface tension time scale brings up the decaying oscillation stage closer in time. Overall, figure 2 suggests that there is no single most amplified wavenumber $\widehat{k}$, and hence the stability should be interpreted in terms different from those in standard eigenvalue studies. The purpose of the subsequent discussion is to disentangle the observed dynamics.

3.2. *Long-wave approximation*

To get a better sense of the system behaviour, let us consider a long-wave, $kF \ll 1$, and long-time, $t \gg t_c$, approximation. Introducing $u_n = \widehat{f}_n' \exp(\int a\,\mathrm{d}t/2)$, we can

https://doi.org/10.1017/jfm.2017.535 Published online by Cambridge University Press

reduce (2.8) to

$$u_n'' - s^2(t)u_n = 0, \quad \text{where } s^2(t) = -b + \tfrac{1}{2}a_t + \tfrac{1}{4}a^2. \tag{3.3}$$

Depending upon the index n of the Bessel function, we obtain

$$n = 0\colon\ s^2(t) = \frac{1}{4t^2} + \frac{k^2}{2F}\frac{\sigma}{\rho}(1 - k^2F^2) + \frac{1}{4}\left(\frac{Q}{4\pi}k^2\right)^2, \tag{3.4a}$$

$$n \neq 0\colon\ s^2(t) = \frac{n}{4t^2} + \frac{n}{F^3}\frac{\sigma}{\rho}(1 - n^2 - k^2F^2), \tag{3.4b}$$

which should be contrasted to the classical dispersion relation for $F = \text{const.}$,

$$s^2 = \frac{\sigma}{\rho}\frac{1}{F^3}\frac{kFI_n'(kF)}{I_n(kF)}(1 - n^2 - k^2F^2), \tag{3.5}$$

with the asymptotics in the long-wave approximation,

$$n = 0\colon\ s^2 \simeq \frac{\sigma}{\rho}\frac{k^2}{2F}(1 - k^2F^2), \quad n \neq 0\colon\ s^2 \simeq \frac{\sigma}{\rho}\frac{n}{F^3}(1 - n^2 - k^2F^2), \tag{3.6a,b}$$

where now s has the meaning of a growth rate (eigenvalue), i.e. $\widehat{f_n'} \sim \mathrm{e}^{st}$: for $n = 0$ (axisymmetric mode), the growth is observed for $k^2F^2 < 1$, while for $n \geqslant 1$, all modes are stable (not growing). The dispersion relation (3.6) suggests that the growth rate in the classical case vanishes in the limit of $k = 0$ (long waves, for which the surface tension σ is ineffective) and at $k = F^{-1}$ (short waves, when the surface tension starts to suppress instability). Clearly, the long-wave asymptotics is accurate enough to determine the optimal mode n and wavelength k; indeed, expression (3.6) for $n = 0$ gives $kF = 0.707$, versus the precise 0.697 from (3.5). These results are recovered from the time-dependent case (3.4*a*) if one puts $F = \text{const.}$, $Q = 0$ and $t \to \infty$.

In the time-dependent case, when $n = 0$ and $t \to \infty$, we observe that for $k \to 0$, $s^2 = (k^2/2F)(\sigma/\rho) > 0$, i.e. a long-wave instability is expected; for $k \to \infty$, the coefficients in (2.8) become

$$a(t) = \frac{1}{2t}, \quad b(t) = -\frac{1}{2t^2} - \frac{k}{4}\frac{Q}{\pi t}\sqrt{\frac{\pi}{Qt}} - \frac{k\pi}{Qt}\frac{\sigma}{\rho}(1 - n^2 - k^2F^2) \simeq k^3\frac{\sigma}{\rho}, \tag{3.7a,b}$$

so that $s^2(t) = -k^3\sigma/\rho$, i.e. the surface tension has a stabilizing effect on short wavelengths in the long-time limit. Based on the above, one might expect that for some large fixed time t (independent of k), there exists a sufficiently large wavenumber k at which s^2 changes sign from positive to negative and hence, loosely speaking, growth is succeeded by decay in time. While general ordinary differential equation theorems (Bellman 1949; Kamke 1961) applied to (3.3) suggest that instability is plausible, they do not provide any insight into the wavenumber structure of the growing/decaying perturbation. Hence, the rest of this section is devoted to a detailed analysis of the instability phenomena.

https://doi.org/10.1017/jfm.2017.535 Published online by Cambridge University Press

3.3. *Stability time intervals*

Instability develops over several distinct time intervals, defined by the values of Q, σ/ρ and k. In the following analysis, we discuss the solution of (3.3) for $u_0(t)$, bearing in mind that it is related to the total solution via $\widehat{f}_0'(t) = \mathrm{e}^{-t/8t_1}u_0(t)$. In the classical case (3.6), the exponential factor is absent as $t_1 = \infty$. In addition to the mass supply time scale $t_1 = \pi/Qk^2$ previously introduced with $k = F_0^{-1}$, the surface tension time scale $t_2 = (Q/\pi)^3(\rho/\sigma)^2$ emerges. We focus on axisymmetric disturbances, $n = 0$, as the most unstable ones in order to analyse the time intervals on which different terms in (3.4*a*) dominate.

Case 1: $((Q/8\pi)k^2)^2$ is dominant if

$$t \gg 4t_1 \quad \text{and} \quad t \gg 4^5 t_1^2 t_2^{-1} \quad \text{and} \quad t \ll 4^{-5}t_2, \tag{3.8a–c}$$

which is possible provided that t_2 is large enough and t_1 is sufficiently small. In this case, we get a linear oscillator equation with the solution

$$u_0(t) = C_1\mathrm{e}^{(Q/8\pi)k^2 t} + C_2\mathrm{e}^{-(Q/8\pi)k^2 t}; \tag{3.9}$$

i.e. exponential growth of $u_0(t)$ is observed, with the most unstable wavenumber being $k = \infty$ (short waves), which is expected as surface tension is not present in this limit; of course, the conditions (3.8) are invalidated then. However, $\widehat{f}_0'(t)$ (and hence the blob) is not prone to a Rayleigh–Taylor instability; in fact, the acceleration of the interface $F_{tt} \sim -t^{-3/2}$ is negative at this stage. The observed behaviour in this case corresponds to the flat part of the graphs in figure 2(*c*). The presence of the term $(Qk^2/4\pi)^2/4 = 4^{-3}t_1^{-2}$ is due to the radial acceleration of the cylinder interface, as can be gleaned from (2.3).

Case 2: $1/4t^2$ is dominant if

$$t \ll 4t_1 \quad \text{and} \quad t \ll (4^{-1}t_1^2 t_2)^{1/3} \quad \text{and} \quad t \ll (4^{-1}t_1^4 t_2)^{1/5}, \tag{3.10a–c}$$

which is possible provided that both t_1 and t_2 are large enough, i.e. the behaviour corresponds to the earlier time growth in figure 2(*a*). Since in this case $s^2(t) = 1/(4t^2)$, we get Euler's equation, admitting the solution

$$u_0(t) = C_1 t^{(1/2)+(1/\sqrt{2})} + C_2 t^{(1/2)-(1/\sqrt{2})}, \tag{3.11}$$

i.e. algebraic growth is observed.

Case 3: $(k^4/2)(\sigma/\rho)F$ is dominant if

$$t \gg t_1 \quad \text{and} \quad t \gg 4^{-5}t_2 \quad \text{and} \quad t \gg (4^{-1}t_1^4 t_2)^{1/5}, \tag{3.12a–c}$$

which is possible provided that both t_1 and t_2 are small enough. In this case, the solution can be expressed in terms of Bessel functions of fractional order ν, namely

$$u_0(t) = \sqrt{t}Z_{1/2q}\left(\frac{\mathrm{i}}{q}\sqrt{c}t^q\right), \quad \text{where } \frac{1}{2q} = \frac{2}{5},\ c = -\frac{k^4}{2}\frac{\sigma}{\rho}\sqrt{\frac{Q}{\pi}}, \tag{3.13}$$

and $Z_\nu(z) = C_1J_\nu + C_2J_{-\nu}$, with the asymptotics for large z (large time t),

$$J_\nu(z) = \sqrt{2/\nu z}\cos\left[z - (2\nu+1)\pi/4\right] + O(z^{-3/2}) \quad \text{as } z \to \infty. \tag{3.14}$$

Hence, $u_0(t) \sim t^{-1/8}\cos(\alpha t^{5/4}) + \cdots \to 0$ as $t \to +\infty$.

https://doi.org/10.1017/jfm.2017.535 Published online by Cambridge University Press

Case 4: $(k^2/2F)(\sigma/\rho)$ is dominant if

$$t \ll t_1 \quad \text{and} \quad t \ll 4^5 t_1^2 t_2^{-1} \quad \text{and} \quad t \gg (4^{-1} t_1^2 t_2)^{1/3}, \tag{3.15a–c}$$

which is possible provided that t_1 is large enough and t_2 is sufficiently small. In this case, $s^2(t) = ct^{-1/2}$, with $c = 2^{-1} t_1^{-1} t_2^{-1/2}$, and thus

$$u_0 = t^{1/2} Z_{1/3}\left(\tfrac{4}{3} \mathrm{i} c^{1/2} t^{3/4}\right), \tag{3.16}$$

where $Z_\nu(z) = C_1 J_\nu(z) + C_2 J_{-\nu}(z)$, $z = \mathrm{i}\alpha t^{3/4}$ and $\alpha = (4/3)c^{1/2}$, with the asymptotics $u_0(t) \sim t^{-3/8} \mathrm{e}^{\alpha t^{3/4}}$. Hence, the solution first grows (case 4) and then decays in an oscillating fashion (case 3) in time, as observed in figures 2(*a–c*). Thus, the combination of cases 3 and 4 is analogous to the classical situation (3.6), and therefore one then might infer that selection of the most amplified wavenumber k should be made possible when two terms – $(k^2/2F)(\sigma/\rho)$ and $(k^4/2)(\sigma/\rho)F$ – compete, similarly to the classical Rayleigh–Plateau instability. However, this expectation proves to be unfeasible.

3.4. *On non-existence of optimal growth time and wavenumber*

Here, we will consider cases 3 and 4 together (omitting index 0), which leads to the equation

$$u'' - s^2(t) u = 0, \quad s^2(t) = \frac{\alpha}{\sqrt{t}} - \beta\sqrt{t}, \quad \text{with } \alpha = \frac{k^2}{2}\frac{\sigma}{\rho}\sqrt{\frac{\pi}{Q}},\ \beta = \alpha\frac{k^2 Q}{\pi}. \tag{3.17a,b}$$

The sign of $s^2(t)$ changes at the 'turning' point t_*, which coincidentally equals the previously introduced inertial time scale $t_* = \alpha/\beta \equiv t_1$. The solution to this problem is amenable to the Wentzel–Kramers–Brillouin method, namely away from the turning point it renders

$$u(t) = \frac{C_\pm}{[s^2(t)]^{1/4}} \exp\left[\pm \int_{t_0}^{t} \sqrt{s^2(\tau)}\, \mathrm{d}\tau\right], \tag{3.18}$$

which after Taylor expansion of $s^2(t)$ near t_*, $s^2(t_* + t) = -\alpha t/t_*^{3/2} + \cdots$, with t now measured from the turning point t_*, becomes

$$t > 0\colon\ u = \frac{t_*^{3/8}}{(\alpha t)^{1/4}}[A \mathrm{e}^{\mathrm{i}(2/3)(\alpha^{1/2}/t_*^{3/4})t^{3/2}} + B \mathrm{e}^{-\mathrm{i}(2/3)(\alpha^{1/2}/t_*^{3/4})t^{3/2}}], \tag{3.19a}$$

$$t < 0\colon\ u = \frac{t_*^{3/8}}{(-\alpha t)^{1/4}}[C \mathrm{e}^{-(2/3)(\alpha^{1/2}/t_*^{3/4})(-t)^{3/2}} + D \mathrm{e}^{(2/3)(\alpha^{1/2}/t_*^{3/4})(-t)^{3/2}}], \tag{3.19b}$$

where $D = 0$, as for $t \to -\infty$, the solution should be bounded.

In a neighbourhood of the turning point, (3.17) simplifies to the Airy equation

$$u'' + \alpha t t_*^{-3/2} u = 0, \tag{3.20}$$

the solution of which is expressed in terms of Airy functions $u_0(t) = a\,\mathrm{Ai}(z) + b\,\mathrm{Bi}(z)$, $z = -\alpha^{1/3} t_*^{-1/2} t$. In order to determine the constants a and b, we will need the asymptotics of Ai and Bi for $z \gg 1 (t \to -\infty)$ and $-z \gg 1 (t \to +\infty)$ (Abramowitz & Stegun 1965). Matching these asymptotics with the Wentzel–Kramers–Brillouin

https://doi.org/10.1017/jfm.2017.535 Published online by Cambridge University Press

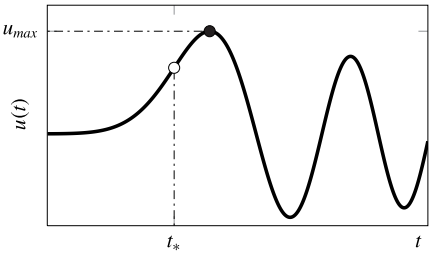


FIGURE 3. Solution of (3.17) near the turning point t_*; the maximum is achieved after passing through t_*.

solutions (3.19) for both $t \to \pm\infty$, we find

$$A = \frac{e^{i(\pi/4)}}{2\sqrt{\pi}} \frac{\alpha^{1/6}}{t_*^{1/4}}[b - ia], \quad B = \frac{e^{-i(\pi/4)}}{2\sqrt{\pi}} \frac{\alpha^{1/6}}{t_*^{1/4}}[b + ia], \quad C = \frac{a}{2\sqrt{\pi}} \frac{\alpha^{1/6}}{t_*^{1/4}}, \quad D = \frac{b}{\sqrt{\pi}} \frac{\alpha^{1/6}}{t_*^{1/4}}. \tag{3.21a–d}$$

Since $D = 0$, then $b = 0$. As a result, the solution for $t > 0$, i.e. after the turning point t_*, reads

$$u(t) = C \frac{2t_*^{3/8}}{\alpha^{1/4} t^{1/4}} \sin\left(\xi + \frac{\pi}{4}\right), \quad \text{where } \xi = \frac{2}{3} \frac{\alpha^{1/2}}{t_*^{3/4}} t^{3/2}, \tag{3.22}$$

and thus the interfacial deflection becomes $\widehat{f'}(t) = e^{-1/2 \int a\,dt} u(t) = \text{const.}\, e^{-t/8t_*} u(t)$, where again t is defined relative to the turning point t_*. To determine the maximum achieved during the time evolution, we differentiate the above (total) solution,

$$\frac{d}{dt}[e^{-t/8t_*} u(t)] = 0 \Rightarrow \frac{1}{6} \tan\left(\xi + \frac{\pi}{4}\right)[\delta \xi^{2/3} + 1] = \xi, \quad \delta = \frac{3^{2/3}}{2^{4/3}} \left(\frac{t_2}{t_1}\right)^{1/6} \ll 1, \tag{3.23a,b}$$

where $\delta \ll 1$ since $t_2/t_1 \ll 1$ in the considered case 4. For $\delta = 0$, the above extremum condition admits the approximate solution reflecting the presence of infinitely many 'humps' (cf. figure 3),

$$\xi_0 = \pi\left(m + \frac{1}{4}\right) - \xi', \quad \xi' = \frac{2}{3\pi} \frac{1}{1 + 4m}, \quad m \in \mathbb{Z}. \tag{3.24a,b}$$

The corresponding maxima of $u(t)$ scale as $u_{max} \sim m^{-1/6} k^{-5/6}$ for $m \gg 1$, i.e. the extremum decays with m. For $\delta \neq 0$, the solution of (3.23) is corrected to $\xi = (1 - 3\delta/2)\xi_0$; that is, the time when the maximum of the solution is reached becomes shorter with increase of the ratio t_2/t_1.

Finally, in order to determine the wavenumber for which the maximum of the solution is absolute, it should be noticed that this maximum corresponds to $m = 1$ and is achieved after passing through the turning point t_*, cf. figure 3, which is analogous to the bifurcation delay phenomena in dynamical systems if $s^2(t)$ is deemed to be a time-dependent bifurcation parameter. Given the general turning point solution with $b = 0$, we can first determine where the maximum is achieved,

$$\frac{d}{dt}[e^{-t/8t_*} \mathrm{Ai}(\tau)] = 0 \Rightarrow \frac{\mathrm{Ai}(-\theta\widetilde{\tau})}{\mathrm{Ai}'(-\theta\widetilde{\tau})} = -8\theta, \quad \theta = \frac{1}{2^{1/3}} \left(\frac{t_1}{t_2}\right)^{1/6}, \ \tau = \frac{t}{t_1}, \tag{3.25}$$

https://doi.org/10.1017/jfm.2017.535 Published online by Cambridge University Press

with $\theta \gg 1$ in case 4. Graphical analysis indicates that the solution of the above equation is near the first zero of $\mathrm{Ai}'(-\theta\,\widetilde{\tau})$, denoted by $a_s' = -1.01879\cdots < 0$ (Abramowitz & Stegun 1965), which allows one to apply asymptotic methods to find the solution of (3.25),

$$\widetilde{\tau} = -\frac{a_s'}{\theta} + \widetilde{\tau}', \quad \text{where } \widetilde{\tau}' = -\frac{1}{8\theta^2}\frac{\mathrm{Ai}(a_s')}{\mathrm{Ai}''(a_s')} + \cdots. \tag{3.26}$$

By evaluating the solution at $\widetilde{\tau}$, i.e. $\widehat{f}'(\widetilde{\tau}) = \text{const.}\, t_2^{1/2}\theta^{5/6}\mathrm{e}^{-\widetilde{\tau}/8}\mathrm{Ai}(-\theta\,\widetilde{\tau})$, it is straightforward to show that there is no 'optimum' wavenumber k. Indeed, as $k \to 0$,

$$\widehat{f}'(\widetilde{\tau}) \sim \theta^{5/6} \sim k^{-5/18}, \tag{3.27}$$

because $\mathrm{Ai}(-\theta\widetilde{\tau}) \sim \text{const.}$ and $\mathrm{e}^{-\widetilde{\tau}/8} \sim 1$ (since $t_1 \to +\infty$ for $k \to 0$). As expected from the discussion in § 3.1, there is no critical self-similar wavenumber scaled with $F^{-1}(t)$ and growing exponentially since, based on (3.26) and (3.27), the most amplified wavenumber at a given time t scales as $k \sim t^{-3/5}$. Thus, the fundamental difference from the classical case $Q = 0$ is that no matter how small (but non-zero) k is, there is a large enough time when this k is amplified and then damped (for later times). It should be noted that for $k \equiv 0$, from (3.4*a*) we find that $a(t) = 0$, $b(t) = -1/(4t^2)$ and $s^2(t) = 1/(4t^2)$, so that the leading-order solution reads as

$$u(t) = C_1 t^{(1/2)+(1/\sqrt{2})} + C_2 t^{(1/2)-(1/\sqrt{2})}, \quad \text{and therefore } \widehat{f}' \sim t^{(1/2)+(1/\sqrt{2})}, \tag{3.28a,b}$$

i.e. it grows faster than the undisturbed interface $F \sim t^{1/2}$, in analogy with the Rayleigh–Taylor instability of an expanding sphere (Plesset 1954). The result (3.28) for $k \equiv 0$ contrasts with $\widehat{f}' \sim t^{1/6}$ for $k \to 0$, i.e. the limits $k \to 0$ and $t \to \infty$ are not interchangeable and thus distinguished. Since the limit of $k = 0$ corresponds to a 2D problem, this transition from 3D to 2D makes some of the mechanisms (transfer of energy from the base state to the perturbation) disappear. Physically, a growing blob imminently breaks up in a finite time, and thus the range of finite non-zero wavenumbers amplified on this time scale ultimately affects the size of the resulting drops, which might be non-uniform due to the lack of a single preferred wavenumber.

4. Effects of lateral acceleration

In addition to the radial acceleration due to $Q \neq 0$, there could also be a lateral acceleration, e.g. due to the presence of gravity or, as in the case of a retracting soap film, due to the force pulling the cylinder in one direction. In the latter case, however, the Bond number $Bo = \rho F_0^2 g/\sigma$ at the start of retraction (when the acceleration is the largest) of a film of thickness h is not small as $Bo = F_0/h \geqslant 1$; this is easy to see from the estimate of acceleration based on the Taylor–Culick theory, $g \sim \sigma/(\rho h F_0)$. The case of low Bond numbers in the soap film retraction corresponds only to the later stage of retraction when the blob has already grown and the acceleration diminishes as the blob approaches a constant Taylor–Culick speed $\sqrt{2\sigma/\rho h}$, but by that time, the blob instability may have already developed. Here, we focus on the case of a weak acceleration due to external body forces such as gravity, so that $Bo \ll 1$, which nevertheless leads to a modification of the base state and a contribution to the instability growth, analysed below with the help of (2.8).

https://doi.org/10.1017/jfm.2017.535 Published online by Cambridge University Press

4.1. *Base state correction*

From (2.8), it is obvious that non-zero acceleration g affects mode $n = 1$ only and thus induces a non-axisymmetric flow field in the blob such as in figure 1(*c*),

$$L\widehat{f}_1' = gF/2, \tag{4.1}$$

which after the transformation $u_1 = \widehat{f}_1' \exp(\int a\,\mathrm{d}t/2)$ reduces to

$$u_1'' - s^2(t)u_1 = Ct^{1/2}gF(t) \equiv h(t), \quad \text{where } s^2(t) = t^{-2}[4^{-1} - (t/t_2)^{1/2}k^2F^2]. \tag{4.2}$$

Looking for a long-time correction, we can simplify $s^2(t)$ to $s^2(t) = -t^{-1/2}t_2^{-1/2}t_{-1} < 0$, provided that $t \gg 4^{2/3}t^{2/3}t_2^{1/3}$. The solution for the homogeneous part of (4.2) is

$$u_1(t) = \sqrt{t}Z_{2/3}\left(\tfrac{4}{3}t_1^{-1/2}t_2^{-1/4}t^{3/4}\right), \tag{4.3}$$

where $Z_\nu(z) = C_1J_\nu(z) + C_2J_{-\nu}(z)$, $z = \gamma t^{3/4}$, $\gamma = (4/3)t_1^{-1/2}t_2^{-1/4}$ and $\nu = 2/3$. If $u_1 = C_1v_1 + C_2v_2$, with $v_1 = t^{1/2}J_\nu(z)$ and $v_2 = t^{1/2}J_{-\nu}(z)$, then the Wronskian is $w = v_1v_2' - v_2v_1'$ and the solution to the inhomogeneous problem (4.2) reads

$$u_1(t) = v_2(t)\int^t \frac{v_1(\tau)h(\tau)}{w(\tau)}\,\mathrm{d}\tau - v_1(t)\int^t \frac{v_2(\tau)h(\tau)}{w(\tau)}\,\mathrm{d}\tau. \tag{4.4}$$

Since we are considering the long-time limit, given the asymptotics (3.14), we can choose as independent solutions $v_1 = t^{1/8}\mathrm{e}^{\mathrm{i}\gamma t^{3/4}}$ and $v_2 = t^{1/8}\mathrm{e}^{-\mathrm{i}\gamma t^{3/4}}$, so that the Wronskian becomes constant, $w = -3\mathrm{i}\gamma/2$, and the long-time limit of the solution (modulo a constant coefficient) is

$$u_1(t) \sim t^{1/8}\mathrm{e}^{\mathrm{i}\gamma t^{3/4}}\int^t \tau^{9/8}\mathrm{e}^{-\mathrm{i}\gamma\tau^{3/4}}\,\mathrm{d}\tau - t^{1/8}\mathrm{e}^{-\mathrm{i}\gamma t^{3/4}}\int^t \tau^{9/8}\mathrm{e}^{\mathrm{i}\gamma\tau^{3/4}}\,\mathrm{d}\tau \sim t^{3/2}, \tag{4.5}$$

where we took into account that the leading-order contribution of the integrals in the above expression can be evaluated through integration by parts,

$$\int^t \tau^{9/8}\mathrm{e}^{\mathrm{i}\gamma\tau^{3/4}}\,\mathrm{d}\tau = -\mathrm{i}\frac{4}{3\gamma}t^{11/8}\mathrm{e}^{\mathrm{i}\gamma t^{3/4}} + O(t^{5/8}). \tag{4.6}$$

As a result, the correction to the base state scales with time t, acceleration g and mass flux Q as $u_1 \sim g\sqrt{Q}t^{3/2}$. For shorter times, i.e. when $1/(4t^2)$ dominates in $s^2(t)$, it is still the same mode $n = 1$ that is excited, but with a different time exponent.

4.2. *Contribution to instability*

Since lateral acceleration acts at all times, it makes sense to consider its contribution to instability at early times – if it boosts it, the effect will be observable. From (2.8), we see that the axisymmetric mode is affected by mode one through the presence of acceleration g,

$$L\widehat{f}_0' = g(\widehat{f}_{-1}' + \widehat{f}_1')/2 = g\widehat{f}_1', \tag{4.7}$$

where we took into account the symmetry $n \to -n$ and $\widehat{f}_1'$ is determined from the homogeneous equation $L\widehat{f}_1' = 0$ or, after the transformation $\widehat{f}_1' = \exp(-\int a\,\mathrm{d}t/2)u_1 = t^{-1/2}u_1$ corresponding to $a(t) = 1/t$, from (3.3) with $n = 1$. For short times, $s^2(t) = 1/(4t^2)$, and hence the leading-order solution of (3.3) is $u_1(t) \sim t^{(1/2)+(1/\sqrt{2})}$,

https://doi.org/10.1017/jfm.2017.535 Published online by Cambridge University Press

so that $\widehat{f}_1' \sim t^{1/\sqrt{2}}$. To construct the solution to (4.7), we make the transformation $u_0 = \widehat{f}_0' \exp(\int a\,\mathrm{d}t/2)$, where $a = 1/(4t_1)$, to produce

$$u_0'' - s^2(t)u_0 = \mathrm{e}^{-t/8t_1} g\widehat{f}_1'/2 \equiv h(t) \sim g\mathrm{e}^{-t/8t_1} t^{1/\sqrt{2}}. \tag{4.8}$$

Since for short times $s^2(t) = 1/(4t^2)$, two independent solutions of the homogeneous part are

$$u_0(t) = C_1 v_1 + C_2 v_2, \quad \text{with } v_1(t) = t^{(1/2)+(1/\sqrt{2})},\ v_2(t) = t^{(1/2)-(1/\sqrt{2})}, \tag{4.9}$$

i.e. given by case 2, and the Wronskian $w = -\sqrt{2}$. Using formula (4.4), the corresponding perturbation driven by acceleration g is then to leading order given by $u_0(t) \sim g\mathrm{e}^{-t/8t_1} t^{1+(1/\sqrt{2})}$, i.e. $\widehat{f}_0' = t^{1+(1/\sqrt{2})}$, and thus the (algebraic) growth is faster than that in the absence of acceleration, which is $t^{(1+\sqrt{2})/2}\mathrm{e}^{t/8t_1}$. Here, the exponential should be discarded as $t \ll t_1$ according to the case 2 assumptions. Hence, the presence of lateral acceleration entails amplification of the instability at early times without changing the wavenumber structure of the perturbation.

5. Discussion and further questions

In this paper, we considered the case in which the time scale for the growth of the liquid blob is commensurate with the intrinsic time scale for the instability in the static situation, so that quasistatic analyses and the idea of a time-varying critical wavenumber fail. Linearization of the basic equations about the axisymmetric base state produces a non-autonomous non-homogeneous oscillator equation (2.8). The results show that no matter how small the wavenumber k is, the apparent growth of the corresponding mode is illusory, as all of the modes ultimately evolve to decaying oscillations after passing through a turning point in time t_* at which the time-dependent 'spring constant' $s^2(t)$ changes sign. Furthermore, this time increases unboundedly for $k \to 0$. Qualitatively, the ultimate decay of the perturbation can be predicted from the classical theory, in which the unstable wavelengths $\lambda = 2\pi/k$ correspond to $\lambda > 2\pi F$, i.e. should be greater than the circumference of the blob. If at a given instant of time a perturbation of a particular wavelength λ^* in that range is expected to grow, at later time it is pushed back to the stable range $\lambda^* < 2\pi F(t)$ due to the growth of $F(t)$. Hence, several 'standard' assumptions based on the direct translation of the classical theory onto the time-varying case – exponential growth of perturbations and time-varying wavenumber – are generally invalid. These seemingly counterintuitive results can be foreseen from the simple fact that in 3D, in general, there is no conformal (i.e. angle preserving) mapping that leaves the Laplace equation (2.1*a*) invariant. The exceptions – translations and homogeneous scalings, rotations and reflections, and inversions – known from Liouville's theorem (Blair 2000) obviously do not apply to the growing cylindrical blob considered here, thus making the presented theory non-conformal (Blumenhagen & Plauschinn 2009). If such a mapping – between a growing and a static blob problem – parameterized by time t were to exist, then there would also exist a most unstable wavenumber that scales with time.

Therefore, a growing blob is expected to rupture in a manner different from a static blob with one preferred wavelength. In the natural scenario, when one starts with random initial conditions with no preferred wavelength, then a range of wavelengths, determined by the time scale of the cylinder rupture (or, at least, by the time it

https://doi.org/10.1017/jfm.2017.535 Published online by Cambridge University Press

takes for the amplitude of perturbations to become finite and comparable to the cylinder radius, thus triggering nonlinear mechanisms), will be amplified. Since perturbations with different wavelengths in this range would also have random phase shifts between them, then the resulting drop sizes should not be uniform. In the other scenario, when one provides an initial modulation with a particular wavelength, such as in the experiments of Donnelly & Glaberson (1966), who verified the classical dispersion relation (3.5), the breakup may result in a uniform size of the drops. At this point, there are no experiments (yet) which would be directly comparable to the offered theory. The closest phenomena would be along-the-edge instability of retracting soap films, but, as was mentioned above, the Bond numbers in that case are greater than or equal to one at the start of retraction. The case of low Bond numbers in the soap film retraction corresponds only to the later stage of retraction when the blob is already massive and the acceleration decreases as the blob approaches a constant Taylor–Culick speed, but by that time an instability would have already developed. Should the presented theory be applicable in that case, it would predict that the lateral acceleration would amplify the instability at early times without changing the wavenumber structure of the perturbation. Any future experiment would have to deliver sufficiently high-fidelity data to be able to distinguish non-exponential growths predicted by the theory and, instead of focusing on an average wavelength of perturbation as commonly done, pay attention to the large scatter around the average, which is indicative of a range of wavelengths amplified, thus leading to breakup at different drop sizes. It would also be interesting to observe, e.g. through an initial modulation, the wavenumbers that initially grow and then decay in an oscillating fashion as in figure 2.

In conclusion, it is worth noting that the transient growth of the perturbation observed in figure 2 is a consequence of both the non-normal and non-autonomous nature of the linear operator of the homogeneous part of (2.7). Once the perturbation amplitude becomes finite, nonlinear advection terms $(\boldsymbol{v}\cdot\boldsymbol{\nabla})\boldsymbol{v}$ in the Euler equations must be taken into account, which affect not only the amplitude of the disturbance, but also its direction, due to the gradient operator $\boldsymbol{\nabla}$, thus influencing the eventual breakup process. All of these aspects are beyond the scope of the present analysis. While the case of $Q=\text{const.}$ considered in detail here provides a roadmap to the instability development for a growing cylindrical blob, it would also be interesting to extend the present study to a time-varying mass flux $Q=Q(t)$, in particular to understand the stability of time-periodic $Q(t)$ amenable to Floquet analysis and to find a way to suppress instability by controlling the form of $Q(t)$. Moreover, the influence of viscosity has been omitted in the present analysis, although its inclusion should not be a serious undertaking in the linear approximation (Levich 1962). Finally, evaluation of the effect of displacement of the line source off the symmetry axis, while expected to enhance instability because the amplitude of I_n increases towards the surface where the Rayleigh–Plateau instability is generated, would be important for quantitative understanding of various problems such as retracting liquid (soap) sheets, where the coupling between the liquid sheet and the rim in previous works (e.g. Agbaglah *et al.* 2013) is usually considered through the variation of the rim radius only, i.e. without actual interaction between the rim and the sheet.

Acknowledgements

This work was partially supported by a National Science Foundation (NSF) CAREER award under grant no. 1054267 and the Natural Sciences and Engineering Research Council of Canada (NSERC) under grant no. 6186. The author would also like to thank A. Zelnikov for stimulating discussions.

https://doi.org/10.1017/jfm.2017.535 Published online by Cambridge University Press

References

ABRAMOWITZ, M. & STEGUN, I. A. 1965 *Handbook of Mathematical Functions*. Dover.

AGBAGLAH, G., JOSSERAND, C. & ZALESKI, S. 2013 Longitudinal instability of a liquid rim. *Phys. Fluids* **25**, 022103.

BELLMAN, R. 1949 A survey of the theory of the boundedness, stability, and asymptotic behaviour of solutions of linear and nonlinear differential and difference equations. *Tech. Rep.* NAVEXOS P-596. Office of Naval Research, Washington DC.

BLAIR, D. E. 2000 *Inversion Theory and Conformal Mapping*. AMS.

BLUMENHAGEN, R. & PLAUSCHINN, E. 2009 *Introduction to Conformal Field Theory*. Springer.

CULICK, F. E. C. 1960 Comments on a ruptured soap film. *J. Appl. Phys.* **31**, 1128–1129.

DAVIS, S. H. 1976 The stability of time-periodic flows. *Annu. Rev. Fluid Mech.* **8**, 57–74.

DONNELLY, R. J. & GLABERSON, W. 1966 Experiments on the capillary instability of a liquid jet. *Proc. R. Soc. Lond.* A **290**, 547–556.

DRAZIN, P. G. & REID, W. H. 2004 *Hydrodynamic Stability*. Cambridge University Press.

DZIWNIK, M., KORZEC, M., MÜNCH, A. & WAGNER, B. 2014 Stability analysis of unsteady, nonuniform base states in thin film equations. *Multiscale Model. Simul.* **12**, 755–780.

FULLANA, J. M. & ZALESKI, S. 1999 Stability of a growing end rim in a liquid sheet of uniform thickness. *Phys. Fluids* **11**, 952–954.

HOMSY, G. M. 1973 Global stability of time-dependent flows: impulsively heated or cooled fluid layers. *J. Fluid Mech.* **60**, 129–139.

KAMKE, E. 1961 *Handbook of Ordinary Differential Equations*. Fizmatgiz.

KRECHETNIKOV, R. 2010 Stability of liquid sheet edges. *Phys. Fluids* **22**, 092101.

LEVICH, V. G. 1962 *Physicochemical Hydrodynamics*. Prentice-Hall.

PLESSET, M. S. 1954 On the stability of fluid flows with spherical symmetry. *J. Appl. Phys.* **25**, 96–98.

RAYLEIGH, LORD 1878 On the instability of jets. *Proc. Lond. Math. Soc.* **10**, 4–13.

ROISMAN, I. V., HORVAT, K. & TROPEA, C. 2006 Spray impact: rim transverse instability initiating fingering and splash, and description of a secondary spray. *Phys. Fluids* **18**, 102104.

TAYLOR, G. I. 1959 The dynamics of thin sheets of fluid. III. Disintegration of fluid sheets. *Proc. R. Soc. Lond.* A **253**, 313–321.

https://doi.org/10.1017/jfm.2017.535 Published online by Cambridge University Press